Published in final edited form as:
Toxicol Lett. 2012 November 15; 214(3): 288–295. doi:10.1016/j.toxlet.2012.09.008.

Effect of Divalent Metals on the Neuronal Proteasomal System, Prion Protein Ubiquitination and Aggregation

A. G. Kanthasamy[*], **C. Choi**, **H. Jin**, **D.S. Harischandra**, **V. Anantharam**, and **A. Kanthasamy**
Department of Biomedical Sciences, Iowa Center for Advanced Neurotoxicology, Iowa State University, Ames, IA 50011, USA (A.G.K., C.C, H.J., D.S.H., V.A., A.K.)

Abstract

The role of normal cellular prion protein (PrP) remains to be fully elucidated; however, the protein is crucial for the infection and progression of prion diseases. Recent evidence indicates that PrP is a metalloprotein since the octapeptide repeat sequences in the protein have high affinity for various divalent cations and the binding sites appear to play a role in the pathogenesis of prion diseases. In our present study, we tested several divalent metals including manganese and cadmium and determined their effects on protein degradation and protein aggregation in mouse neuronal cells expressing PrP protein. Cadmium was more neurotoxic than manganese following 24 h exposure. Manganese did not show any significant effect on the inhibition of proteasomal activity or formation of high molecular weight ubiquitinated PrP proteins. Interestingly, treatment with cadmium profoundly inhibited proteasomal activity, which resulted in greatly increased formation of high molecular weight ubiquitinated PrP proteins. Immunohistochemical analysis also revealed a dramatic increase in formation of oligomers after cadmium treatment. Cadmium also increased the formation of ubiquitinated prion PrP, but it did not lead to the formation of proteinase-K resistant PrP. Collectively, our results show that a divalent metal, cadmium affects proteasomal function and prion protein aggregation, which promote neurotoxicity.

Keywords

metals; proteasome dysfunction; protein aggregation; manganese; neurotoxicity

1. Introduction

Transmissible spongiform encephalopathies (TSE) in humans, as well as in other animals, are caused by conformational change of normal prion protein (PrP^{C}) into abnormal prion protein (PrP^{Sc}). PrP^{Sc} has a tendency to aggregate into fibrils, is highly resistant to digestion by proteinase-K, and carries an infectious element. The exact mechanism of conformational change remains to be determined, but theoretical models of template assisted changes and seed based changes have been proposed (Stohr et al., 2008). The normal form of PrP^{C} is

[*]Corresponding author: Dr. Anumantha G. Kanthasamy, Distinguished Professor and Lloyd Chair, Parkinson's Disorder Research Laboratory, Iowa Center for Advanced Neurotoxicology, Department of Biomedical Sciences, 2062 Veterinary Medicine Building, Iowa State University, Ames, IA 50011, USA Phone: 01-515-294-2516; Fax: 01-515-294-2315; akanthas@iastate.edu.

Conflict of interest
There are no conflicts of interest to declare.

expressed ubiquitously in the central nervous system, the peripheral nervous system, and to a certain extent the immune system (Prinz et al., 2003). And although the exact function of these proteins remains elusive, they are required in the infection and propagation of the TSEs (Raeber et al., 1997). Studies have shown altered metal content in the brains of animals infected with TSE, which supports the hypothesis that TSEs could be caused by metal imbalances in the brain (Singh et al., 2009; Thackray et al., 2002).

The normal form of prion protein is predominantly α-helical in structure, attached to the surface of cells via the glycosyl phosphatidyl inositol (GPI) anchor. The C-terminal regions are highly structured, with two N-linked glycosylations. The N-terminal is rather unstructured, with four octapeptide repeat regions (PHGGGWGQ) and His 96 and 106, which have high binding affinity to divalent cations (Jackson et al., 2001). Copper in particular has been found to directly interact with these sites, and causes a rapid turnover of PrP^{C}, strongly pointing to the role of PrP^{C} in copper metabolism (Brown, 2004; Brown et al., 1997; Pushie et al., 2011). Other divalent cations have been associated with the same sites, but have weaker affinities (Gaggelli et al., 2005; Jackson et al., 2001). Manganese may replace copper in the octapeptide repeat region of the PrP^{C} and alter the structure of the protein (Brazier et al., 2008; Brown et al., 2000; Wong et al., 2001). Furthermore, elevated levels of manganese have been observed in blood and brain samples from humans infected with the prion disease Creutzfeldt-Jakob Disease (CJD), mice infected with scrapie, and cattle infected with bovine spongiform encephalopathy (BSE) (Hesketh et al., 2008; Hesketh et al., 2007; Thackray et al., 2002; Wong et al., 2001). Interestingly, our laboratory has previously demonstrated that normal cellular prion can interact with manganese to protect cells against manganese neurotoxicity at early stages of manganese exposure (Anantharam et al., 2008; Choi et al., 2007). We also reported that manganese significantly increases cellular prion protein levels by altering the stability of prion protein (Choi et al., 2010). Most recently, we found that the conversion of normal prion protein to the pathogenic isoform (PrP^{Sc}) enhances the ability of prion to regulate manganese homeostasis and neurotoxicity in a cell model of prion disease (Martin et al., 2011). All these findings support a crucial involvement of metals in the pathogenesis of prion disease.

One possible mechanism of PrP^{Sc} propagation is the impairment of the proteasomal degradation system (Hilker et al., 2011; Tenzer et al., 2004). PrP^{C} is normally degraded by the proteasomal system, and when the proteasomal system is inhibited, abnormal forms could accumulate in cells (Yedidia et al., 2001). Or alternatively, replacement of copper with different divalent cations could alter prion protein stability, thereby causing accumulation in the cytosol (Di Natale et al., 2005; Stanczak et al., 2005). In either case, we were interested in whether PrP^{C} cells treated with manganese could potentially inhibit proteasomal activity, leading to accumulation of un-degraded PrP^{C}. Interestingly, manganese does not impair proteasomal activity, nor did it cause accumulation of PrP^{C} in our study. However, cadmium, another divalent cation, induced impairment in proteasomal activity and increased the formation of ubiquitinated PrP and oligomers; but inhibition of proteasomal activity did not lead to the formation of proteinase-K resistant forms of PrP^{C}.

2. Materials and Methods

2.1. Chemicals

CdCl2, β-actin and phenylmethylsulphonylfluoride (PMSF) were purchased from Sigma (St. Louis, MO); Bradford protein assay kit was purchased from Bio-Rad Laboratories (Hercules, CA). DMEM (Dulbecco's modified eagle medium), fetal bovine serum, L-glutamine, penicillin, Trypsin/EDTA, and streptomycin were purchased from Invitrogen (Gaithersburg, MD); proteinase-K was purchased from Promega (Madison, WI);

monoclonal mouse anti-PrP (3F4) antibody recognizing sequences 109 through 112 in hamster and human PrP was purchased from Signet Labs (Berkeley, CA).

2.2. In vitro cell culture model

Mouse neural progenitor cells expressing prion protein (PrP^C) were kindly provided by Dr. Suzette A. Priola, Rocky Mountain Lab, NIAIDS, Montana and cultured as described previously (Chesebro et al., 1993; Takemura et al., 2006). The cells were derived from the CF10 mouse neural cell line lacking prion protein and engineered to stably express the mouse PrP^C gene with the 3F4 hamster epitope. Cells were harvested into phosphate buffered saline (PBS) and resuspended in either homogenization buffer (20 mM Tris-HCl, pH 8.0, 2 mM EDTA, 10 mM EGTA, 2 mM DTT, 1 mM PMSF, 25 μg/ml aprotinin, and 10 μg/ml leupeptin) and sonicated, or lysed in lysis buffer (0.5 % Triton X-100, 0.5 % sodium deoxycholate, 5 mM Tris-HCl, 150 mM NaCl, 5 mM EDTA in PBS pH 7.4). For preparation of soluble and insoluble cell fractions, low detergent lysis buffer (20 mM Tris/HCl, pH 8.0, 10 mM EGTA, 2 mM EDTA, 2 mM dithiothreitol, 1 mM phenylmethysulfonyl fluoride, 25 μg/ml aprotinin, and 10 μg/ml leupeptin, 0.5% Triton X-100) was used to collect the soluble fraction by centrifugation, and insoluble lysis buffer (20 mM Tris/HCl, pH 8.0, 10 mM EGTA, 2 mM EDTA, 2 mM dithiothreitol, 1 mM phenylmethysulfonyl fluoride, 25 μg/ml aprotinin, and 10 μg/ml leupeptin, 0.5% Triton X-100, 2% SDS) was used to resuspend the pellet to obtain the insoluble fraction.

2.3. Measurement of cell viability

Cell death was determined using the Trypan Blue exclusion method. The cells were grown in 6 well plates, and then treated with various concentrations of cadmium for 24 h. For time dependent cell death, cells were treated with cadmium for 24 and 48 h. Afterwards, the cells were removed using Trypsin/EDTA and rinsed once with PBS before resuspending samples in PBS. These cells were counted using a hemocytometer. The calculation of live cells was as follows: number of live cells divided by total number of live cells in untreated control.

2.4. Proteasomal peptidase activity assay

The proteasome enzymatic assay was performed as described previously (Sun et al., 2005). In brief, after treatment, cells were collected, washed and lysed in hypotonic buffer (10 mM HEPES, 5 mM $MgCl_2$, 10 mM KCl, 1% sucrose, and 0.2% CHAPS). The lysates were then incubated with fluorogenic substrates for Chymotrypsin-like activity (75 μM Suc-LLVY-AMC, Calbiochem, San Diego CA) and Peptidyl-Glutamyl-Peptidase Hydroxylase (PGPH)-like activity (75 μM Z-LLE-AMC, Calbiochem, San Diego, CA) in assay buffer (50 mM Tris-HCl, 20 mM KCL, 5 mM magnesium acetate, and 10 mM dithiothreitol, pH 7.6) at 37°C for 30 min. The cleaved fluorescent product was measured at excitation wavelength of 380 nm and emission wavelength of 460 nm using a fluorescent plate reader (Gemini XS, Molecular Devices, Sunnyvale, CA). The enzymatic activity was normalized to the protein concentrations using the Bradford protein assay.

2.5. Western blot analysis

Low detergent soluble and insoluble fractions were separated according to a procedure described previously with slight modifications (Sun et al., 2005). After exposure to cadmium, manganese, or MG-132, a non-specific proteasome inhibitor, cells were collected and washed once with ice cold PBS. The cell pellets were suspended in low detergent lysis buffer. The lysates were ultracentrifuged at 100,000 X g for 40 min. The detergent soluble fraction was obtained by collecting the resulting supernatant. The detergent insoluble pellets were washed once with the lysis buffer and resuspended in insoluble lysis buffer, and sonicated for 20 s. Equal amounts of protein were loaded in 8% SDS-polyacrylamide gel, as

determined by the Bradford protein assay. Proteins were transferred to nitrocellulose membranes and blocked with 5% nonfat dry milk in Tris buffered solution with 1% Tween-20 (TBST). The membranes were probed with ubiquitin antibody (1:500; DAKO Cytomation, Carpenteria, CA) overnight at 4°C and incubated with horseradish peroxidase (HRP) conjugated secondary anti-rabbit or anti-mouse IgG (1:2000 dilution; Amersham, Piscataway, NJ) for an additional 1 h prior to detection with an ECL kit (Amersham, Piscataway, NJ). Images were captured with a Kodak 2000 MM (New Haven, CT) imaging system. The same membrane was reprobed with anti-mouse β-actin (1:5000 dilution).

2.6. Immunofluorescence staining

Immunofluorescence staining was performed as described previously (Kaul et al., 2005). Mouse neuronal cells were grown on coverslips pre-coated with poly-L-lysine and treated with cadmium. Cells were washed once with PBS, and fixed in 4% paraformaldehyde. After fixation, slides were washed three times with PBS, and incubated with blocking buffer (5% bovine serum albumin, 5% goat serum in PBS) to block nonspecific sites. For oligomer (A11, Biosource International, Camarillo, CA) and prion (3F4, Signet Laboratories, Dedham, MA) primary antibody binding, fixed cells were incubated in the same blocking buffer with 0.1% Triton X-100. Following primary antibody incubation, slides were washed thoroughly with PBS and fluorochrome conjugated secondary antibody incubation was performed in the blocking buffer. Nucleic stain was performed with Hoechst 33342 at a concentration of 10 μg/ml. After final nucleic staining, the fixed cells were washed with PBS and mounted onto a slide with Prolong (Invitrogen, Carlsbad, CA) anti-fade reagent mounting medium. The images were viewed by fluorescent microscopy (Nikon TE2000) and captured using a SPOT digital camera.

2.7. Limited proteolysis of PrP

Prion protein resistance to proteinase-K digestion was determined as previously described, with slight modifications (Priola et al., 1994). For *in vitro* incubation, cells were either treated with 10 μM cadmium or untreated. After a 48 h incubation period, cells were collected and washed once with PBS. Lysis buffer was added to the pellet and vortexed. Clarified cell lysates were obtained by centrifugation at 16,000 X g for 10 min. Proteinase-K was added to the cell lysates at a final concentration of 1 μg/ml and incubated at 37°C for selected time points. To stop the digestion, PMSF was added to a final concentration of 4 mM, and sample loading buffer was added to the digested lysates prior to analysis by Western blot (section 2.5).

2.8. Dot blot analysis

Formation of protein oligomers was determined by dot blot measurements using anti-rabbit A11 antibody, which recognizes oligomers of proteins independent of amino acid sequences. Dot blot analysis using this antibody has been used for identification of protein oligomers in various models of neurodegenerative disorders. The procedure for the dot blot assay was followed, as described by the manufacturer. Briefly, cadmium-treated cells were collected after 24 and 48 h and suspended in homogenization buffer. After protein concentrations were determined with the Bradford assay, 10 μg of cell lysates were spotted on the nitrocellulose membrane and allowed to air dry for at least 30 min. Membranes were then blocked with 5% nonfat dry milk in TBST for 1 h, followed by 3 washing steps (15 min each). Then, the membranes were incubated with A11 anti-oligomer antibody (dilution 1:2000) for 1 h at RT, and washed 3 times (15 min each). Afterwards, the membrane was treated with HRP conjugated secondary anti-rabbit IgG for 1 h. Antibody bound proteins were detected with an ECL detection kit, and densitometric analysis of the dots representing the oligomeric protein aggregates was performed with Kodak's one-dimensional image analysis software. For detection of oligomer formation in nuclear and cytoplasmic fractions,

the NE-PER Nuclear and Cytoplasmic Extraction Reagents Kit (Thermo Fisher Scientific, Rockford, IL) was used for sample preparation prior to dot blot analysis.

2.9. Immunoprecipitation assay

Immunoprecipitation study was conducted to examine the association between PrP and ubiquitin protein, as previously described with some modifications (Kaul et al., 2005). Briefly, cytosolic protein (400 μg) was immunoprecipitated overnight at 4°C using 10 μg of anti-ubiquitin antibody. The immunoprecipitates were then incubated with protein A Sepharose for 1 h at 4° C. The protein A bound antigen-antibody complex was then washed three times with homogenization buffer, and resuspended in 2X loading buffer. Samples were boiled for 5 min, and then centrifuged prior to analysis by Western blot.

2.10. Data analysis and statistics

Data were analyzed with Prism 4.0 software (GraphPad Software, San Diego, CA). Bonferroni's post-hoc multiple comparison testing was used to delineate significance between cadmium treated groups, the control (untreated), and the manganese treated samples. For densitometric analysis of limited proteolysis, band intensity was normalized to control bands at 0 min, and one-phase exponential decay was fit to the data. Differences greater than $P<0.05$ were considered significant and are indicated with asterisks.

3. Results

3.1. Cadmium is neurotoxic in mouse neuronal cells

Although cadmium is normally not considered a neurotoxicant, cadmium as a divalent cation was used to examine cellular changes in our mouse neuronal cells. Cadmium caused both dose and time dependent cell death in mouse neuronal cells, as measured by the Trypan blue exclusion method (Figure 1A&B). An effective concentration was determined by treating cells with varying concentrations (0–100 μM) of $CdCl_2$ for 24 h. The effective concentration (EC_{50}) was used for time dependent studies as well (Figure 1B). It should also be noted that the choice of the cadmium dose (10 μM) is in line with many published studies related to the action of cadmium on the central nervous system (Chen et al., 2011; Lopez et al., 2006; Xu et al., 2011). As shown in Figure 1B, treatment with 10 μM $CdCl_2$ resulted in a significant decrease ($p<0.01$) in cell viability after 24 and 48 h. Phase-contrast images further show altered cellular morphologies after 10 μM cadmium treatment (Figure 1C). Extended treatment with 10 μM cadmium for 48 h resulted in very low cell viability. The clumps of cells were verified as apoptotic using live cell staining with Sytox® green nucleic dye, which showed a higher number of Sytox positive cells with treatment.

3.2. Cadmium treatment impairs proteasomal activity in mouse neuronal cells

Since PrP has been shown to have affinity for divalent cations, enzymatic activity of 20S/26S proteasome was examined following manganese and cadmium treatment at 24 and 48 h. Fluorogenic substrates for peptidyl glutamyl peptide hydrolase-like activity (PGPH) and chymotrypsin-like activity were used to evaluate the proteasome activity. As shown in Figure 2A, 10 μM cadmium treatment induced a significant decrease ($p<0.001$) in both PGPH and chymotrypsin-like activity at 24 and 48 h. Interestingly, treatment with 30 μM $MnCl_2$ did not result in inhibition of proteasome activity in any of the substrates (Figure 2B). As a positive control for the substrates, MG-132 (non-specific proteasome inhibitor) was used (Figure 2C). Treatment with 5 μM MG-132 for 3 h resulted in a significant decrease ($p<0.001$) in both substrates. Our recent findings demonstrated that intracellular manganese level was significantly increased in 30 and 100 μM manganese-treated PrP^c cells compared to untreated cells, indicating that these cells can effectively take up manganese (Choi et al., 2007). It has been also reported that both manganese and cadmium are taken up

by neurons via voltage-gated Ca^{2+} channels (Narita et al., 1990; Usai et al., 1999). Manganese also enters the cells via divalent cation metal transporters (DMT) in neuronal cells (Dobson et al., 2004). Further, we tested whether treatment with low doses of cadmium could also impair proteasomal activity. As shown in Figure 2D, dose studies indicated that incubation with 5 μM cadmium for 48 h resulted in a modest but significant reduction ($p<0.05$) in both PGPH and chymotrypsin-like activity, whereas proteasomal activity was not or only marginally affected by lower doses (1 to 3 μM) of cadmium. Together, these results show that cadmium effectively inhibits proteasomal activity in mouse neuronal cells; however, manganese was not as effective as cadmium at inhibiting proteasome activity.

3.3. Cadmium treatment results in accumulation of high molecular weight ubiquitinated proteins

Most proteins are tagged with ubiquitin prior to degradation by proteasomes, and impaired proteasomal activity can lead to accumulation of high molecular weight ubiquitinated proteins. This is attributed to reduced clearance of ubiquitinated proteins by the proteasome. As shown in Figure 3, cadmium-induced impairment of proteasome activity resulted in accumulation of high molecular weight ubiquitinated proteins in both soluble and insoluble fractions. As compared to untreated controls, both 24 and 48 h treatment with cadmium resulted in a significant increase in ubiquitinated proteins (second and third lanes, respectively) in both soluble and insoluble fractions. Although a visible difference in the insoluble fractions between 24 and 48 h cadmium treatment was not observed, there seems to be a slight increase in ubiquitinated proteins for the 48 h cadmium treatment as compared to the 24 h cadmium treatment in the soluble fraction. Whereas, treatment with another divalent metal manganese did not show any accumulation of high molecular weight ubiquitinated proteins in either the soluble or the insoluble fractions (data not shown). Proteasome inhibitor MG-132 was used a positive control. Treatment with MG-132 also resulted in a slight increase in ubiquitinated proteins in both soluble and insoluble fractions (fourth lane). Equal protein loading was confirmed with β-actin.

3.4. Cadmium induces formation of soluble oligomers, but not Proteinase-K resistant prion proteins

Many neurodegenerative disorders are associated with accumulation of misfolded proteins. Recent development of A11 anti-oligomer antibody, which recognizes amino acid sequence independent oligomers of proteins, has enabled the determination of protein oligomers in neurodegenerative models. To further verify protein aggregation induced by cadmium, cells were treated with cadmium for 24 and 48 h and stained (Figure 4). Without treatment, oligomers were not detected; however, with cadmium treatment, increased fluorescence of oligomers was observed. The greater amount of oligomers observed seems to correspond to the duration of treatment. For quantitative analysis, the amount of oligomer formation was detected using the dot blot technique (Figure 5A). Increased dot intensity was seen at both 24 and 48 h of cadmium treatment; 10% and 50% increase in oligomer formation was observed, respectively. Below the graph is a representative dot blot image of control, cadmium treatment for 24 h, and cadmium treatment for 48 h. To verify the cellular location of oligomer formation, nuclear and cytoplasmic fractions were obtained from the samples for analysis by dot blot (Figure 5B & 5C). As seen with the quantification of dot blot intensity, there was no observable difference in the nuclear fraction of control or cadmium treated samples (Figure 5B). However, analysis of the cytoplasmic fraction indicates a clear and significant difference in the amount of oligomers that was detected with cadmium treatment (Figure 5C).

To examine whether the altered proteasomal function and increased oligomer formation resulted in prion protein with altered susceptibility to proteinase-K, cell lysates were

subjected to limited proteolysis (Figure 6). As seen in the figure, cadmium treatment did not result in formation of prion proteins resistant to proteinase-K digestion. As seen in Figure 6A, limited proteolysis following cadmium treatment did not result in altered susceptibility of PrP^{C} to proteolytic digestion as compared to control. To verify that the proteolytic capability of proteinase-K was not altered, the same samples were also probed with β-actin (Figure 6B). Data points from normalized densitometric analysis were fit to one-phase exponential decay, and a kinetic rate profile was obtained (Table 1). Together, these data show that cadmium treatment results in increased formation of oligomers, but not of formation of prion proteins that are resistant to proteinase-K digestion.

3.5. Cadmium increases formation of ubiquitinated prion proteins

Studies have shown that the prion protein is degraded via the ubiquitin degradation pathway (Ma and Lindquist, 2001). It is logical that impairment of the proteasome would lead to accumulation of ubiquitinated proteins, which would include prion proteins. To verify that the prion protein was ubiquitinated following cadmium treatment, cell lysates were immunoprecipitated with ubiquitin antibody, and analyzed by Western blot (Figure 7A). Imunoprecipitated prion protein was detected using prion protein antibody (3F4). As seen in the Western blot analysis, the amount of ubiquitination was significantly increased following cadmium treatment for 48 h in all three glycosylated forms of prion protein (Figure 7B). Cadmium treatment for 24 h did not significantly alter the amount of ubiquitination of prion protein for any of the glycosylated forms.

4. Discussion

Mounting evidence points to a role of ubiquitinated proteins in many neurological diseases, and prion disease is no exception (Ciechanover and Brundin, 2003; Lehman, 2009; Mayer, 2003; Olanow and McNaught, 2011). PrP^{C} has been shown to be degraded by the ubiquitin mediated proteasome pathway (Tenzer et al., 2004), and protease resistant PrP or PrP^{Sc} is also ubiquitinated before undergoing degradation through the proteasome pathway (Kang et al., 2004). In brains of infected animals, increased ubiquitin immunoreactivity has been observed (Kang et al., 2004; Kristiansen et al., 2005). Since endogenous prion protein is degraded *via* cellular degradative processes, impairment of the proteasomal system could contribute to the initiation and/or progression of the disease (Cohen and Taraboulos, 2003).

PrP has been shown to be possess metal binding sites with high affinity for divalent cations involved in normal cellular function (Jackson et al., 2001). There has been speculation that replacement of copper with other divalent cations could potentially alter the structure of the PrP, thereby contributing to the formation of PrP^{Sc} (Nishina et al., 2004; Wong et al., 2004). It has been demonstrated in a previous study that rat astrocytes incubated with manganese for prolonged periods generate proteinase-K resistant forms of PrP (Brown et al., 2000). Other folding studies have suggested that PrP could adopt a secondary structure more closely resembling PrP^{Sc} in the presence of manganese, pointing to the possible role of other metals replacing copper (Treiber et al., 2006). Thus, we wanted to examine whether inhibition of the ubiquitin proteasomal system by divalent cations manganese and cadmium could lead to increased accumulation of abnormal PrP.

In our *in vitro* cell culture model, we observed that manganese did not impair proteasomal activity. Cadmium, on the other hand, significantly impaired proteasomal activity. The cadmium-induced impairment of proteasomal function led to increased formation of insoluble and soluble ubiquitinated proteins. Using A11 antibody, we also observed that cadmium treatment induced a significant increase in levels of soluble oligomers. However, unlike manganese (Choi et al., 2010), cadmium did not induce formation of proteinase-K resistant PrP. These results suggest several possibilities. One possibility is that replacement

of copper with a different divalent cation could alter the conformation of PrP, targeting it for degradation. Further, an increased generation of targeted proteins could impair the proteasome function, thereby increasing the possibility of excessive abnormal PrP in the cytosol. Another possibility is that PrP^{Sc} naturally exists in homeostasis with PrP^{C}, and lack of PrP^{Sc} found in normal organisms could be due to the high degradation rate associated with PrP^{Sc}. If the degradative system were impaired by inhibition of proteasomal activity, accumulation of abnormal PrP could lead to an infectious state. It should be noted that, in the present study, we used only we used only 30 μM manganese, which did not produce any significant toxicity under these conditions. This is consistent with our previous study, in which we determined the EC50 for manganese was 118 μM in the mouse neural cell model (Choi et al., 2007). Although manganese did not show an effect on proteasomal activity, we recently reported that manganese increased stability of prion protein possibly by interacting with octapeptide binding sites in the protein (Choi et al., 2010). Thus, the elevated levels of manganese observed in the samples of humans infected with the prion disease may have a role in stabilization and propagation of prion protein. It is also noteworthy that an increased prion mRNA in non-neuronal rat PC12 pheochromocytoma cells by cadmium treatment has been reported (Varela-Nallar et al., 2006). However, such effect was not observed in our neural cells (data not shown), suggesting that cadmium induced prion accumulation in neuronal cells is mainly due to the inhibition of protein degradation pathway.

Speculation as to whether proteasome inhibition leads to prion disease has increased (Aguzzi and Steele, 2009; Kristiansen et al., 2005). Treatment with a non-specific proteasome inhibitor (MG-132) induces formation of insoluble PrP in N2a cells (Fioriti et al., 2005). These formations of insoluble PrP were not toxic to the cells. Although accumulation of PrP in the cytosol was observed, perturbations of PrP metabolism through the proteasome pathway probably do not induce pathogenic PrP^{Sc}. However, chronic impairment of proteasome function resulting in accumulation of insoluble of PrP could lead to a pathogenic form of PrP. We observed that treatment with cadmium resulted in accumulation of high molecular weight ubiquitinated proteins in both soluble and insoluble fractions. Although both 24 and 48 h treatment with cadmium resulted in increased formation of high molecular weight ubiquitinated proteins, immunoprecipitation studies revealed that PrP was significantly ubiquitinated only at 48 h.

Cadmium is a heavy metal with highly toxic effects, and its accumulation in the human body is known to induce many severe health effects, including cancer and central nervous system (CNS) disorders (Minami et al., 2001). Both occupational exposure and food are the major routes of environmental cadmium exposure (Minami et al., 2001). Further, cadmium has a biological half-life ranging from 10 to 30 years, is relatively water soluble compared to other heavy metals, and therefore has the potential to bioaccumulate in various tissues and cells including neuronal tissues. Thus, a better understanding of cadmium-induced neurotoxicity may eventually lead to development of mechanism-based treatment strategies.

Together, our results suggest that certain metals can impair proteasomal function in neural cells, leading to increased ubiquitination of proteins and cell death. Although the cellular mechanism of cadmium induced proteasomal dysfunction is not clear, ubiquitinated PrP clearly accumulated during cadmium exposure. These findings suggest the possibility that altered metal homeostasis in the brain may contribute to impaired prion protein degradation via proteasomal inhibition.

Acknowledgments

This work was supported by National Institutes of Health Grants ES19276 and ES10586. The W. Eugene and Linda Lloyd Endowed Chair for AGK is also acknowledged.

References

Aguzzi A, Steele AD. Prion topology and toxicity. Cell. 2009; 137:994–996. [PubMed: 19524502]

Anantharam V, Kanthasamy A, Choi CJ, Martin DP, Latchoumycandane C, Richt JA, Kanthasamy AG. Opposing roles of prion protein in oxidative stress- and ER stress-induced apoptotic signaling. Free radical biology & medicine. 2008; 45:1530–1541. [PubMed: 18835352]

Brazier MW, Davies P, Player E, Marken F, Viles JH, Brown DR. Manganese binding to the prion protein. J Biol Chem. 2008; 283:12831–12839. [PubMed: 18332141]

Brown DR. Role of the prion protein in copper turnover in astrocytes. Neurobiol Dis. 2004; 15:534–543. [PubMed: 15056461]

Brown DR, Hafiz F, Glasssmith LL, Wong BS, Jones IM, Clive C, Haswell SJ. Consequences of manganese replacement of copper for prion protein function and proteinase resistance. Embo J. 2000; 19:1180–1186. [PubMed: 10716918]

Brown DR, Qin K, Herms JW, Madlung A, Manson J, Strome R, Fraser PE, Kruck T, von Bohlen A, Schulz-Schaeffer W, Giese A, Westaway D, Kretzschmar H. The cellular prion protein binds copper in vivo. Nature. 1997; 390:684–687. [PubMed: 9414160]

Chen S, Xu Y, Xu B, Guo M, Zhang Z, Liu L, Ma H, Chen Z, Luo Y, Huang S, Chen L. CaMKII is involved in cadmium activation of MAPK and mTOR pathways leading to neuronal cell death. J Neurochem. 2011; 119:1108–1118. [PubMed: 21933187]

Chesebro B, Wehrly K, Caughey B, Nishio J, Ernst D, Race R. Foreign PrP expression and scrapie infection in tissue culture cell lines. Dev Biol Stand. 1993; 80:131–140. [PubMed: 8270103]

Choi CJ, Anantharam V, Martin DP, Nicholson EM, Richt JA, Kanthasamy A, Kanthasamy AG. Manganese upregulates cellular prion protein and contributes to altered stabilization and proteolysis: relevance to role of metals in pathogenesis of prion disease. Toxicological sciences : an official journal of the Society of Toxicology. 2010; 115:535–546. [PubMed: 20176619]

Choi CJ, Anantharam V, Saetveit NJ, Houk RS, Kanthasamy A, Kanthasamy AG. Normal cellular prion protein protects against manganese-induced oxidative stress and apoptotic cell death. Toxicological sciences : an official journal of the Society of Toxicology. 2007; 98:495–509. [PubMed: 17483122]

Ciechanover A, Brundin P. The ubiquitin proteasome system in neurodegenerative diseases: sometimes the chicken, sometimes the egg. Neuron. 2003; 40:427–446. [PubMed: 14556719]

Cohen E, Taraboulos A. Scrapie-like prion protein accumulates in aggresomes of cyclosporin A-treated cells. Embo J. 2003; 22:404–417. [PubMed: 12554642]

Di Natale G, Grasso G, Impellizzeri G, La Mendola D, Micera G, Mihala N, Nagy Z, Osz K, Pappalardo G, Rigo V, Rizzarelli E, Sanna D, Sovago I. Copper(II) interaction with unstructured prion domain outside the octarepeat region: speciation, stability, and binding details of copper(II) complexes with PrP106–126 peptides. Inorg Chem. 2005; 44:7214–7225. [PubMed: 16180886]

Dobson AW, Erikson KM, Aschner M. Manganese neurotoxicity. Annals of the New York Academy of Sciences. 2004; 1012:115–128. [PubMed: 15105259]

Fioriti L, Dossena S, Stewart LR, Stewart RS, Harris DA, Forloni G, Chiesa R. Cytosolic prion protein (PrP) is not toxic in N2a cells and primary neurons expressing pathogenic PrP mutations. J Biol Chem. 2005; 280:11320–11328. [PubMed: 15632159]

Gaggelli E, Bernardi F, Molteni E, Pogni R, Valensin D, Valensin G, Remelli M, Luczkowski M, Kozlowski H. Interaction of the human prion PrP(106–126) sequence with copper(II), manganese(II), and zinc(II): NMR and EPR studies. J Am Chem Soc. 2005; 127:996–1006. [PubMed: 15656638]

Hesketh S, Sassoon J, Knight R, Brown DR. Elevated manganese levels in blood and CNS in human prion disease. Mol Cell Neurosci. 2008; 37:590–598. [PubMed: 18234506]

Hesketh S, Sassoon J, Knight R, Hopkins J, Brown DR. Elevated manganese levels in blood and central nervous system occur before onset of clinical signs in scrapie and bovine spongiform encephalopathy. Journal of animal science. 2007; 85:1596–1609. [PubMed: 17296770]

Hilker R, Brotchie JM, Chapman J. Pros and cons of a prion-like pathogenesis in Parkinson's disease. BMC neurology. 2011; 11:74. [PubMed: 21689433]

Jackson GS, Murray I, Hosszu LL, Gibbs N, Waltho JP, Clarke AR, Collinge J. Location and properties of metal-binding sites on the human prion protein. Proc Natl Acad Sci U S A. 2001; 98:8531–8535. [PubMed: 11438695]

Kang SC, Brown DR, Whiteman M, Li R, Pan T, Perry G, Wisniewski T, Sy MS, Wong BS. Prion protein is ubiquitinated after developing protease resistance in the brains of scrapie-infected mice. J Pathol. 2004; 203:603–608. [PubMed: 15095484]

Kaul S, Anantharam V, Kanthasamy A, Kanthasamy AG. Wild-type alpha-synuclein interacts with pro-apoptotic proteins PKCdelta and BAD to protect dopaminergic neuronal cells against MPP+-induced apoptotic cell death. Brain Res Mol Brain Res. 2005; 139:137–152. [PubMed: 15978696]

Kristiansen M, Messenger MJ, Klohn PC, Brandner S, Wadsworth JD, Collinge J, Tabrizi SJ. Disease-related prion protein forms aggresomes in neuronal cells leading to caspase activation and apoptosis. J Biol Chem. 2005; 280:38851–38861. [PubMed: 16157591]

Lehman NL. The ubiquitin proteasome system in neuropathology. Acta neuropathologica. 2009; 118:329–347. [PubMed: 19597829]

Lopez E, Arce C, Oset-Gasque MJ, Canadas S, Gonzalez MP. Cadmium induces reactive oxygen species generation and lipid peroxidation in cortical neurons in culture. Free radical biology & medicine. 2006; 40:940–951. [PubMed: 16540389]

Ma J, Lindquist S. Wild-type PrP and a mutant associated with prion disease are subject to retrograde transport and proteasome degradation. Proc Natl Acad Sci U S A. 2001; 98:14955–14960. [PubMed: 11742063]

Martin DP, Anantharam V, Jin H, Witte T, Houk R, Kanthasamy A, Kanthasamy AG. Infectious prion protein alters manganese transport and neurotoxicity in a cell culture model of prion disease. Neurotoxicology. 2011; 32:554–562. [PubMed: 21871919]

Mayer RJ. From neurodegeneration to neurohomeostasis: the role of ubiquitin. Drug News Perspect. 2003; 16:103–108. [PubMed: 12792671]

Minami A, Takeda A, Nishibaba D, Takefuta S, Oku N. Cadmium toxicity in synaptic neurotransmission in the brain. Brain research. 2001; 894:336–339. [PubMed: 11251212]

Narita K, Kawasaki F, Kita H. Mn and Mg influxes through Ca channels of motor nerve terminals are prevented by verapamil in frogs. Brain research. 1990; 510:289–295. [PubMed: 2158851]

Nishina K, Jenks S, Supattapone S. Ionic strength and transition metals control PrPSc protease resistance and conversion-inducing activity. J Biol Chem. 2004; 279:40788–40794. [PubMed: 15262998]

Olanow CW, McNaught K. Parkinson's disease, proteins, and prions: Milestones. Movement disorders : official journal of the Movement Disorder Society. 2011; 26:1056–1071. [PubMed: 21626551]

Prinz M, Heikenwalder M, Junt T, Schwarz P, Glatzel M, Heppner FL, Fu YX, Lipp M, Aguzzi A. Positioning of follicular dendritic cells within the spleen controls prion neuroinvasion. Nature. 2003; 425:957–962. [PubMed: 14562059]

Priola SA, Caughey B, Raymond GJ, Chesebro B. Prion protein and the scrapie agent: in vitro studies in infected neuroblastoma cells. Infect Agents Dis. 1994; 3:54–58. [PubMed: 7812655]

Pushie MJ, Pickering IJ, Martin GR, Tsutsui S, Jirik FR, George GN. Prion protein expression level alters regional copper, iron and zinc content in the mouse brain. Metallomics : integrated biometal science. 2011; 3:206–214. [PubMed: 21264406]

Raeber AJ, Race RE, Brandner S, Priola SA, Sailer A, Bessen RA, Mucke L, Manson J, Aguzzi A, Oldstone MB, Weissmann C, Chesebro B. Astrocyte-specific expression of hamster prion protein (PrP) renders PrP knockout mice susceptible to hamster scrapie. Embo J. 1997; 16:6057–6065. [PubMed: 9321385]

Singh A, Isaac AO, Luo X, Mohan ML, Cohen ML, Chen F, Kong Q, Bartz J, Singh N. Abnormal brain iron homeostasis in human and animal prion disorders. PLoS pathogens. 2009; 5:e1000336. [PubMed: 19283067]

Stanczak P, Valensin D, Juszczyk P, Grzonka Z, Migliorini C, Molteni E, Valensin G, Gaggelli E, Kozlowski H. Structure and Stability of the Cu(II) Complexes with Tandem Repeats of the Chicken Prion. Biochemistry. 2005; 44:12940–12954. [PubMed: 16185063]

Stohr J, Weinmann N, Wille H, Kaimann T, Nagel-Steger L, Birkmann E, Panza G, Prusiner SB, Eigen M, Riesner D. Mechanisms of prion protein assembly into amyloid. Proc Natl Acad Sci U S A. 2008; 105:2409–2414. [PubMed: 18268326]

Sun F, Anantharam V, Latchoumycandane C, Kanthasamy A, Kanthasamy AG. Dieldrin induces ubiquitin-proteasome dysfunction in alpha-synuclein overexpressing dopaminergic neuronal cells and enhances susceptibility to apoptotic cell death. J Pharmacol Exp Ther. 2005; 315:69–79. [PubMed: 15987830]

Takemura K, Wang P, Vorberg I, Surewicz W, Priola SA, Kanthasamy A, Pottathil R, Chen SG, Sreevatsan S. DNA aptamers that bind to PrP(C) and not PrP(Sc) show sequence and structure specificity. Exp Biol Med (Maywood). 2006; 231:204–214. [PubMed: 16446497]

Tenzer S, Stoltze L, Schonfisch B, Dengjel J, Muller M, Stevanovic S, Rammensee HG, Schild H. Quantitative analysis of prion-protein degradation by constitutive and immuno-20S proteasomes indicates differences correlated with disease susceptibility. J Immunol. 2004; 172:1083–1091. [PubMed: 14707082]

Thackray AM, Knight R, Haswell SJ, Bujdoso R, Brown DR. Metal imbalance and compromised antioxidant function are early changes in prion disease. Biochem J. 2002; 362:253–258. [PubMed: 11829763]

Treiber C, Simons A, Multhaup G. Effect of copper and manganese on the de novo generation of protease-resistant prion protein in yeast cells. Biochemistry. 2006; 45:6674–6680. [PubMed: 16716078]

Usai C, Barberis A, Moccagatta L, Marchetti C. Pathways of cadmium influx in mammalian neurons. J Neurochem. 1999; 72:2154–2161. [PubMed: 10217297]

Varela-Nallar L, Toledo EM, Larrondo LF, Cabral AL, Martins VR, Inestrosa NC. Induction of cellular prion protein gene expression by copper in neurons. American journal of physiology Cell physiology. 2006; 290:C271–281. [PubMed: 16148034]

Wong BS, Chen SG, Colucci M, Xie Z, Pan T, Liu T, Li R, Gambetti P, Sy MS, Brown DR. Aberrant metal binding by prion protein in human prion disease. J Neurochem. 2001; 78:1400–1408. [PubMed: 11579148]

Wong E, Thackray AM, Bujdoso R. Copper induces increased beta-sheet content in the scrapie-susceptible ovine prion protein PrPVRQ compared with the resistant allelic variant PrPARR. Biochem J. 2004; 380:273–282. [PubMed: 14969585]

Xu B, Chen S, Luo Y, Chen Z, Liu L, Zhou H, Chen W, Shen T, Han X, Chen L, Huang S. Calcium signaling is involved in cadmium-induced neuronal apoptosis via induction of reactive oxygen species and activation of MAPK/mTOR network. PloS one. 2011; 6:e19052. [PubMed: 21544200]

Yedidia Y, Horonchik L, Tzaban S, Yanai A, Taraboulos A. Proteasomes and ubiquitin are involved in the turnover of the wild-type prion protein. Embo J. 2001; 20:5383–5391. [PubMed: 11574470]

Research Highlights

- Mouse neuronal cells are more sensitive to cadmium induced neurotoxicity than Mn.
- Cadmium but not Mn inhibits proteasomal activity.
- Cadmium induces accumulation of high molecular weight ubiquitinated proteins.
- Cadmium induces formation of soluble oligomers but not PK resistant prion protein.
- Cadmium promotes neurotoxicity through proteasomal inhibition.

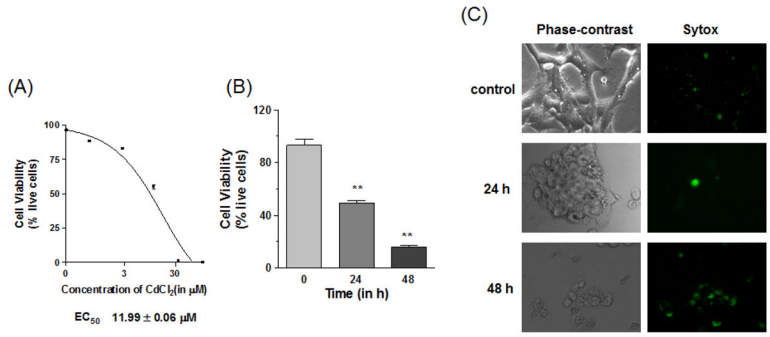

Fig. 1. Cell viability

(A) Dose dependent cadmium-induced cell death. Cells were treated with 0–100 μM $CdCl_2$ for 24 h and cell viability was calculated using the Trypan blue exclusion method. EC_{50} values were calculated with a non-linear regression model. (B) Time dependent cell death induced by cadmium. Cells were treated for 24 and 48 h with 10 μM $CdCl_2$ and cell viability was calculated as described previously. (C) Images of time dependent cell death induced by cadmium. Phase-contrast images were used to observe cell morphologies, while the impermeable nucleic dye Sytox® green was used to observe cells with compromised membranes. All the data were replicated twice in triplicate, **$p<0.01$.

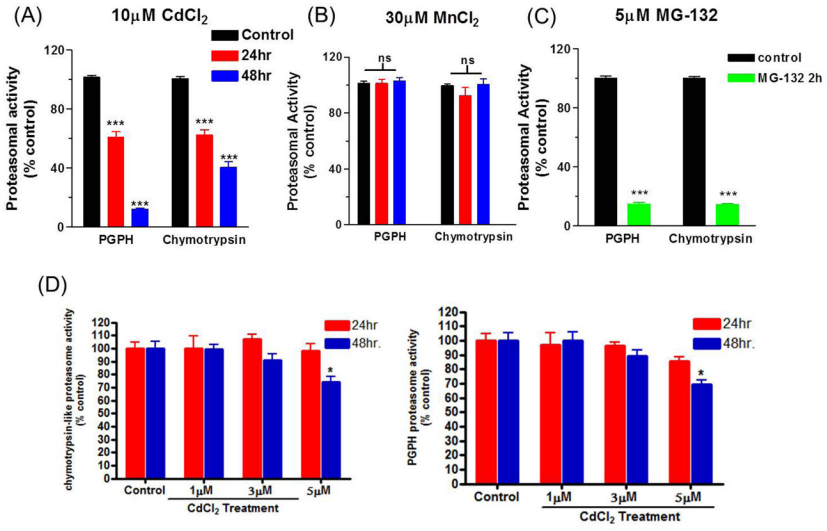

Fig. 2. Measurement of proteasome activity

Cells were treated with 1–10 μM cadmium for 24 and 48 h, and activities of two different proteasomal substrates were examined: peptidyl glutamyl peptidase hydrolase (PGPH)-like activity and chymotrypsin-like activity. (A) Proteasome activity after exposure to 10 μM $CdCl_2$ for 24 and 48 h. (B) Proteasome activity following manganese treatment for 24 and 48 h. (C) Proteasome activity after low doses (1, 3 and 5μM) of $CdCl_2$ treatment for 24 and 48 h. (D) For positive control, cells were treated with MG-132 for 2 h (green bars).*$p<0.05$ and ***$p<0.001$, n=6.

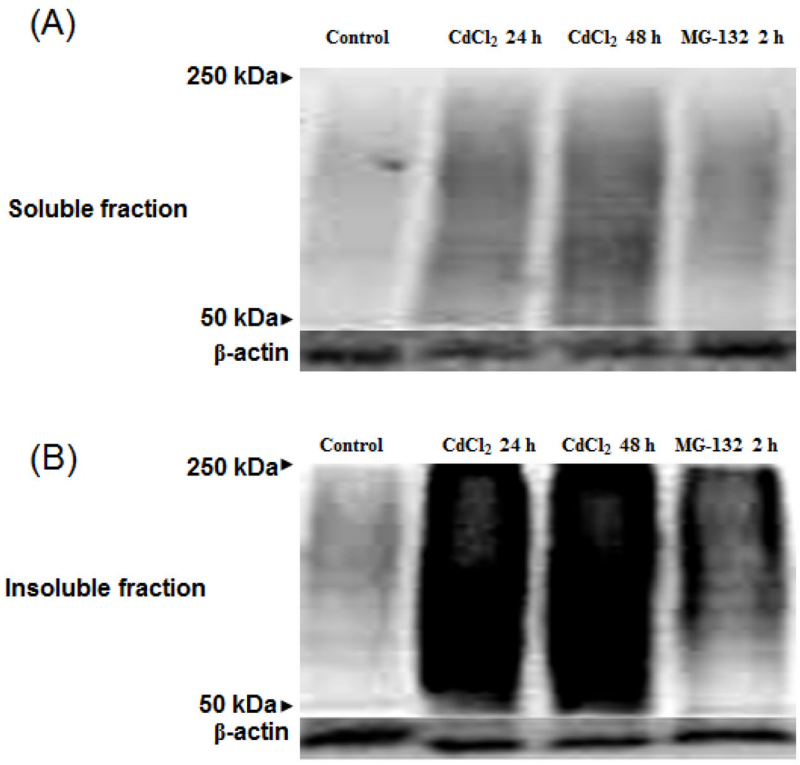

Fig. 3. Detection of high molecular weight ubiquitinated proteins

Soluble (A) and insoluble (B) fractions of cadmium treated cells at 24 and 48 h were analyzed. Positive control cells were treated with 5 μM of MG-132 (non-specific proteasomal inhibitor) for 2 h. Equal protein loading was confirmed with β-actin.

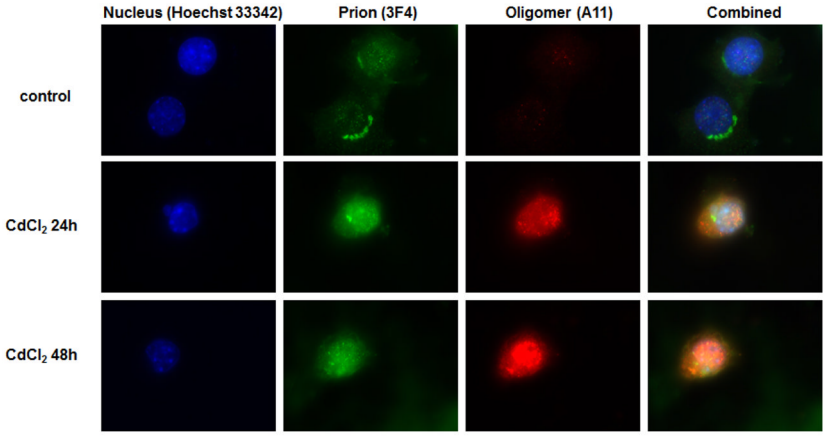

Fig. 4. Detection of oligomer formation following cadmium treatment

Nucleus staining was performed with Hoechst 33342 (blue), prion was detected with 3F4 antibody conjugated to Alexa 488 secondary anti-mouse (green), and oligomer formation was detected with A11 antibody conjugated to Cy3 secondary anti-rabbit (red). Combined images are seen to the far right.

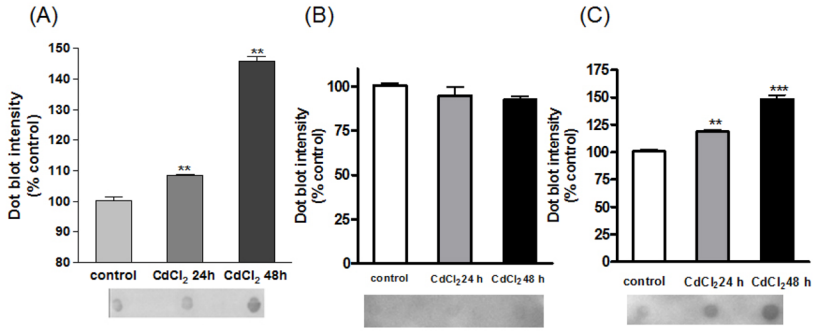

Fig. 5. The amount of oligomer formation was quantified by dot blot assay

Below the graph is a representative image of various treatments: control, cadmium 24 h, and cadmium 48 h treatment, respectively from left to right. (A) Dot blot quantification of total lysates from cadmium treated cells. (B) Dot blot quantification of nuclear fraction in cadmium treated cells. (C) Dot blot quantification of cytoplasmic fraction in cadmium treated cells. **p<0.01, ***p<0.001, n=3.

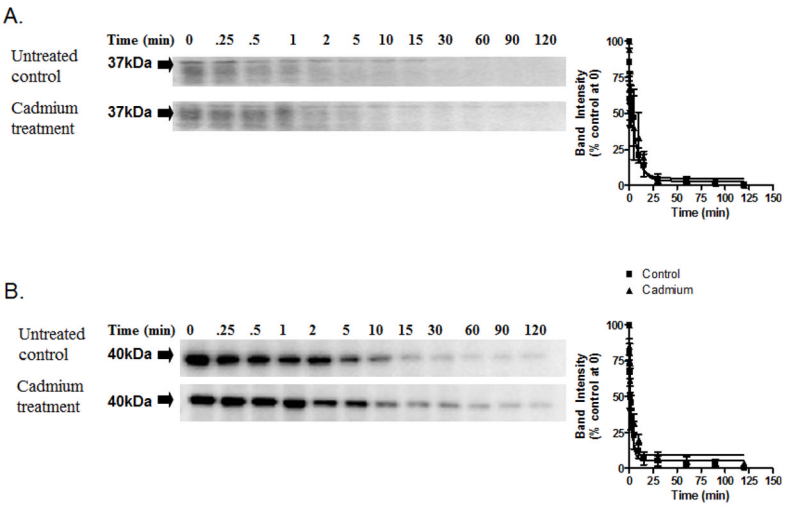

Fig. 6. ***In vitro*** **cadmium treatment does not alter PrPC susceptibility to proteinase-K digestion**

(A) Western blot analysis of limited proteolysis of PrPC in the presence and absence of 10 μM cadmium. (B) Limited proteolysis of β-actin analyzed by Western blot in the presence and absence of cadmium. Kinetic rate profiles of the limited proteolysis of PrPC and β-actin are next to the Western blot images. Each data point represents the mean ± SEM of the normalized band intensity determined by densitometric analysis performed in triplicate. The curve through the data points represents the best fit to a single exponential decay.

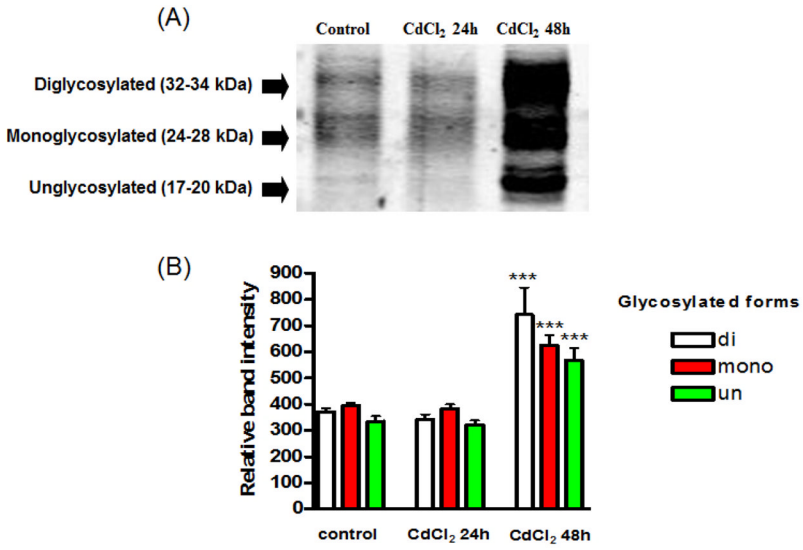

Fig. 7. Immunoprecipitation of prion protein with ubiquitin

(A) Treated and untreated cell lysates were immunoprecipitated with ubiquitin and detected with prion protein antibody (3F4). (B) Three glycosylated forms of prion protein were quantified using the Kodak analysis program. ***p<0.001, n=3.

Table 1

Cadmium treatment does not alter the proteolytic degradation rate of prion protein in an *in vitro* cell culture system. The data were obtained by fitting a single-phase exponential curve onto experiments performed in triplicate, and are represented as mean ± SEM.

	PrP		**β-actin**	
	Untreated	**Cd^{2+} treated**	**Untreated**	**Cd^{2+} treated**
k_{obs}	0.38 ± 0.16	0.35 ± 0.13	0.32 ± 0.13	0.31 ± 0.1
Half-life (min)	1.8 ± 1.2	2.0 ± 1.0	2.2 ± 1.5	2.2 ± 1